Scale effect of corneal adhesion: from solid to membrane

Jiajin Yang
Taiyuan University of Technology
Qiaomei Ren
The First People's Hospital of Jinzhong, Shanxi Medical University
Dong Zhao
Taiyuan University of Technology
Zhipeng Gao (gaozhipeng@tyut.edu.cn)
Taiyuan University of Technology
Xiaona Li
Taiyuan University of Technology
Rui He
Shanxi Eye Hospital
Weiyi Chen
Taiyuan University of Technology

Article

Keywords: Biomechanics, Ophthalmology, Pull-off, JKR theory, Work of adhesion

Posted Date: April 12th, 2022

DOI: https://doi.org/10.21203/rs.3.rs-1532733/v1

Abstract

The adhesion behavior is usually happened in the cornea related to the clinical treatments. Physiologically, an intact natural cornea is inflated by the intraocular pressure. Due to the inflation, the physiological cornea appears the mechanical property likeness to membrane. This characteristic is ignored by the classical theory used to analyze the adhesion behavior of soft solids, such as the Johnson-Kendall-Roberts (JKR) model. Performing the pull-off test, this work evidenced that the classical JKR solution was suitable to calculate the corneal adhesion force when the related contact area was in a smaller size of submillimeter scale. However, when the cornea was contacted in a greater size of millimeter scale, the JKR solutions were clearly smaller than the related experimental data. This error was complemented through modifying the classical JKR model. The modified-JKR model, in this study, was superimposed by the contribution from the surface tension related to the characteristic of membrane. Through the modified-JKR model, the scale effect of the corneal adhesion was realized to describe using a unified theory.

Introduction

The cornea, a transparent organ, forms the anterior pole of the eye, and it plays an essential role in the visual function.[1] Adhesion behavior of cornea is often accompanied with the ophthalmic clinical treatments, such as, wearing contact lenses to correcting myopia.[2,3] After the refractive surgeries, the stabilization of the post-operative cornea depends on the corneal cap firmly adheres to the residual stromal bed.[4] Especially, in terms of corneal transplantation, adhesion is a prominent concern issue of the biocompatibility, the poor interfacial adhesion can affect the clinical outcome of the transplantation.[5] To study the corneal adhesion, therefore, can help us to preferably understand the biomechanics of the cornea associated with the clinical ophthalmology.

Adhesion behavior is usually determined through a pull-off test, that is, a rigid punch indents onto a solid and then detaches from it.[6–10] To analyze the adhesion behavior of a solid, work of adhesion γ, a characteristic of material, must be concerned. There are two classical theories, i.e., Johnson-Kendall-Roberts (JKR)[11] and Derjaguin-Muller-Toporov (DMT)[12] models, used to analyze the adhesion behaviors of the solids. The DMT- and JKR-models describe two different types of separation. They derive two different mathematic formulas used to calculate the adhesion force, i.e., 1.5γπR and 2γπR with R being the derived radius. The DMT-model, related to the strength-limited solution, is suitably used to study the brittle failure; whereas the JKR-model, related to the energy-limited solution, is suited to analyze the ductile failure.[6,13,9] Due to excellent compliance, many previous studies have evidenced that the JKR model is suitable for analyzing the adhesion behaviors of soft materials,[14–16] including cancer cells[17] and biological soft tissues[18].

Indeedly, employing the JKR model, recently Zhu and his colleagues studied and compared the adhesion interactions between the cornea and the silicone contact lenses of different types.[3] Their work focused on

the interfacial adhesion interaction between the two different soft materials, and thus the obtained adhesion force was coupled together with the contributions from the two soft matters. It is difficult to decouple the adhesion force of cornea itself from the interaction associated with the two soft matters. Without decoupling, this work performed the pull-off test to study the corneal adhesion employing the rigid punches, whose stiffness exceeded the cornea more than many orders of magnitude.

Results

Corneal adhesion was not affected by IOP

The experimental results indicated that the corneal adhesion force F_{ad} did not vary with the IOPs. As shown in Fig. 1a, there were no statistical differences existing in the F_{ad} values ($p > 0.05$), obtained by the pull-off test during the cornea under the different IOPs in vitro, except for the comparison between the groups of 40 mmHg and 60 mmHg obtained through the 1mm-R_p punch.

Interestingly, the related calculations of the two parameters, γ and E^*, were like the F_{ad}. As shown in Fig. 1b and 1c, regarding to a punch with a certain radius, the values of γ and E^* did also not vary with the IOPs. There were no statistical differences compared with each other among the different IOP-groups ($p > 0.05$). This phenomenon indicated that the parameters of γ and E^*, obtained here, possessed the intrinsic characteristics of the cornea.

Scale effect of corneal adhesion

To analyze the scale effect of the corneal adhesion, in this study, 20 mmHg and 30 mmHg were selected as the internal environment cornea tolerated, because the normal IOP was approximately ranged from 10 mmHg to 30 mmHg.[19] Under the normal IOP of 20 or 30 mmHg, as shown in Fig. 2, there were scale effect obviously existed in the corneal adhesion. The parameters of γ and E^* exhibited the similar tendency with the function of the punch sizes (Fig. 2a and 2b). For example, under the IOP of 20 mmHg, regarding to the punch with submillimeter sizes (i.e., $R_p \leq 1$ mm), both the two parameters trended to decrease with the increasing of R_p ($p < 0.05$). When the R_p rose to greater than 1 mm, their values trended to without statistical differences ($p > 0.05$), but they were significantly smaller than those obtained by the punch in submillimeter scale ($p < 0.01$).

Additionally, the punch sizes could also assuredly affect the F_{ad}. In the range of R_p from 0.5 mm to 5 mm used here, the experimental data of F_{ad}, trended to gradually rise with the increasing of R_p (Fig. 2c). However, the tendency was very slight when the punch sizes were in the range from 2 mm to 3 mm ($p > 0.05$). Under the IOP of 20 mmHg, for example, the F_{ad} values obtained through the punches with the submillimeter sizes, were obviously significant smaller than those obtained through the greater punches ($p < 0.001$). The minimum value, 1.25 ± 0.25 mN, was obtained by the 0.5mm-R_p punch. It was smaller than that (1.73 ± 0.39 mN) obtained through the 1mm- R_p punch approximately by 28% ($p < 0.01$), and

twofold smaller than that of the maximum value (3.94 ± 0.73 mN) obtained through the 5mm- R_p punch ($p < 0.001$). The related data were detailedly summarized in Table 1.

Table 1. The data of γ, E^*, and F_{ad} obtained from the test performed here.

Radius of punch R_P (mm)								
IOP P (mmHg)		**0.5**	**1**	**2**	**2.5**	**3**	**4**	**5**
γ (mN/mm)	20	0.56 ± 0.19	0.41 ± 0.16	0.29 ± 0.12	0.33 ± 0.15	0.22 ± 0.09	0.23 ± 0.11	0.24 ± 0.09
	30	0.50 ± 0.15	0.46 ± 0.22	0.22 ± 0.11	0.27 ± 0.15	0.22 ± 0.08	0.19 ± 0.11	0.21 ± 0.08
	40		0.47 ± 0.17	0.21 ± 0.08		0.20 ± 0.10	0.18 ±0.09	
	50		0.43 ± 0.17	0.18 ± 0.06		0.18 ± 0.06	0.21 ± 0.10	
	60		0.37 ± 0.13	0.21 ± 0.12		0.20 ± 0.13	0.18 ± 0.08	
E^* (kPa)	20	581.52 ± 275.10	434.18 ± 260.89	437.73 ± 231.14	777.24 ± 500.72	434.92 ± 235.09	407.72 ± 224.77	381.59 ± 161.94
	30	560.80 ± 255.80	449.18 ± 292.02	361.16 ± 184.86	713.89 ± 382.38	441.29 ± 174.80	328.57 ± 145.96	403.92 ± 160.92
	40		601.36 ± 365.53	360.25 ± 182.63		422.27 ± 285.37	363.36 ± 224.58	
	50		558.01 ± 282.76	357.27 ± 247.15		393.64 ± 185.03	395.25 ± 205.55	
	60		492.78 ± 243.71	366.89 ± 237.06		418.69 ± 200.53	377.33 ± 177.10	
F_{ad} (mN)	20	1.25 ± 0.25	1.73 ± 0.39	2.62 ± 0.50	2.62 ± 0.79	2.76 ± 0.46	3.00 ± 0.61	3.94 ± 0.73
	30	1.37 ± 0.43	1.81 ± 0.32	2.47 ± 0.62	2.62 ± 0.79	2.66 ± 0.39	3.00 ± 0.64	3.88 ± 0.87
	40		2.10 ± 0.73	2.56 ± 0.64		2.94 ± 0.47	2.94 ± 0.58	
	50		2.07 ± 0.59	2.42 ± 0.66		2.75 ± 0.38	3.29 ± 0.68	
	60		1.69 ± 0.45	2.74 ± 0.64		2.84 ± 0.49	3.05 ± 0.70	

Analysis employing the JKR models

Substituting the obtained values of γ and E^* into the classical and the modified JKR models, we calculated the F_{ad} values and compared them with the experimental data. The comparisons showed that the classical JKR model should not be adequately used to describe the corneal adhesion, except for the contaction happened in the submillimeter scale.

The experimental data of F_{ad}, as shown in Fig. 3a, were well fitted by the classical JKR solutions when the cornea contacted with the 1mm-R_p punch. However, while the punch with greater sizes (Fig. 3b-3d), such as 3 mm-R_p, the F_{ad} values calculated by the JKR model were much smaller than the experimental data, when the cornea was under the higher IOPs than the normal level (Fig. 3c). Under the IOP of 40 mmHg, for example, the F_{ad} value calculated through the JKR model (1.90 ± 0.76 mN) was smaller than the experimental data (2.94 ± 0.47 mN) approximately by 35% (Fig. 3c). These errors were availably compensated by the modified JKR solutions (Fig. 3b-3d).

The related scale variations described as shown in Fig. 3e-3f and Fig. S5, could evidence the tendency of the corneal adhesion. Compared with the experimental data, both the classical and the modified JKR solutions could obtain the similar tendency functioned by the F_{ad} and R_p. Unlike the modified JKR solutions, however, the related tendency obtained by the JKR solutions was lower than the experimental data. Except for the submillimeter R_p, the JKR solutions were obviously smaller than the one-to-one correspondence experimental F_{ad} values. On the contrary, in terms of the R_p in the millimeter scales, the tendency obtained by the modified JKR solutions was well matched with the experimental data (Fig. 3e-3f).

Discussion

This work reported that the corneal adhesion possessed a scale effect, affected by the contact area. In this study, the classical JKR model, used to describe the adhesion of solids, was valid to analyze the corneal adhesion with the submillimeter sizes (Fig. 3a). However, the validity would decrease with the increasing of the contact area. While the punch sizes were in the millimeter scales, the corneal F_{ad} obtained by the JKR solutions were obviously smaller than the related experimental data (Fig. 3b-3f).

This contradiction, happened between the JKR solutions and the experimental data, implied that the JKR model partially failed in analyzing the corneal adhesion. To find the reason, we deemed that it should be emphasized on the physiology of the natural cornea, which is fully inflated by IOP, like a membrane. To analyze the corneal adhesion, therefore, it should be considered the contribution of the membranous characteristic. This important factor, however, was not considered in the classical JKR model.

According to the comparison results, it was clear that the scale effect of corneal adhesion was associated with its characteristic varied from solid to membrane. In case of the punch size was sufficiently smaller (i.e., submillimeter scale) than the cornea, the cornea should be considered as a solid, and the classical JKR model could obtained the suitable solution (Fig. 3a). Whereas the punch size was

in millimeter scales, the cornea increasingly trended to the characteristic of membrane. Thus, the suitable solution of the corneal adhesion should be obtained by the modified JKR model proposed here.

To simply describe the scale effect of the corneal adhesion, a dimensionless normalization analysis was employed here. The factors, related to the corneal adhesion, contained adhesion force, work of adhesion, elastic modulus, geometry, and IOPs, etc. Taken these factors into account, this work proposed a parameter κ, formulated as Eq. (3), to describe the scale effect.

$$\kappa = \left(\frac{F_{ad}\gamma}{PE^{*}a_c^3} \right)^{\frac{1}{3}}. \quad (3)$$

The parameter of κ, in this study, was described as a function of the ratio between the radii of the punch and the cornea, R_p/R_c. The average value of the corneal radius used here was 9.58 ± 0.22 mm. Compared with the tendencies described in Fig. 3e and 3f, interestingly, the normalization tendencies, functioned with the κ and R_p/R_c, exhibited the opposite (Fig. 4). As shown in Fig. 4, the κ values decreased with the increasing of the ratio R_p/R_c, and the related data were well fitted by an exponential function. For example, in terms of the cornea under the normal IOP of 20 mmHg (Fig. 4a), while the punch was infinitesimal, i.e., the ratio of R_p/R_c boundlessly approaches to zero, the κ value was closer and closer to 1.05, the corneal adhesion increasingly trended to the characteristic of solid. Inversely, while the punch size was infinitely great, it was like that the intact cornea contacted to the ground, the κ value was approximately closer and closer to 0.29, the corneal adhesion increasingly trended to the characteristic of membrane (Fig. 4a). Although the normalization tendencies reversed to the dimensional, the related discrepancies, between the experimental and theoretical data, were the same. Compared with the experimental data, the classical JKR solutions also obtained the lower normalization tendency. And this error also could be offset by the modified JKR solutions (insets in Fig. 4).

Consequently, this work evidenced that the corneal adhesion possessed a scale effect due to its characteristic varied from solid to membrane. While the cornea contacted by a smaller punch in submillimeter, its adhesion could be described by the theory related to solid, i.e., JKR model. While in the greater contact area, however, to analyze the corneal adhesion needed considering the contribution of the surface tension. With the increasing of the contact area, the corneal adhesion increasingly trended to membrane. The related evidences were revealed in the comparison results as shown in Fig. 3, Fig. 4, and Fig. S5. Without wet condition, this study related to the corneal adhesion, also supported the previous discovery of that scale effect was existed in wet adhesion of biological attachment systems.[20]

Clinically, the corneal adhesion usually appeared with the greater contact area in millimeter scale. In terms of the refractive surgeries, for example, the optical operation diameters were in the range of 5–8 mm.[21,22] Additionally, wearing the commercial contact lenses and corneal transplantation, can cover the whole or partial surface of the cornea. To understand the adhesion behavior of cornea itself, this work provided a suitable theory through modifying the classical JKR model.

Compared with the published similar works,[3,23] this present work obtained the F_{ad} values of the cornea were smaller than the previous studies in one or two orders of magnitude. This is because the contact areas observed here, between the cornea and the punch, were much smaller than the previous works related to the cornea contacted with the artificial cornea or the contact lenses.[3,23] The measured F_{ad} value depends on the contact area (Fig. 2). The F_{ad} of the natural cornea was approximately 20 mN, related to the adhesion interaction between the Boston keratoprosthesis and the corneal disk-samples with the radius of 3 mm.[23] However, the maximum critical contact radius a_c, related to the 5 mm-R_p punch with the cornea under 20 mmHg-IOP, obtained here was approximately 0.34 mm (**Table S1**).

In summary, this study evidenced that the corneal adhesion possessed a scale effect. It should be treated as a solid when the cornea contacted in a submillimeter scale, whereas the contaction in a larger size, the characteristic of membrane should be considered in analyzing the corneal adhesion. The modified JKR model proposed here, successfully described the adhesion characteristics of the cornea from solid to membrane.

Methods

Material Preparation

One hundred natural porcine eyes, were consecutively collected from a local slaughterhouse, and were immediately transported to laboratory in two to three hours after slaughter. In laboratory, according to different sizes of the spherical rigid punches, these eyes were divided into seven groups (*supplementary information* **I**) to study the scale effect of corneal adhesion through the pull-off test.

Experimental protocol

The pull-off test, in this study, was performed at room temperature to determine the adhesion behavior of cornea itself. Each eye specimen was indented by the rigid spherical punches (elastic modulus ~ 200 GPa) with different sizes (Fig. 5a and Fig. S1). As shown in Fig. 5a, an eye specimen, exposed its cornea to air, was attached to a fixed chamber, fully filled with phosphate buffer saline (PBS) by negative pressure through an injector, which could simultaneously tune the value of IOP P.

Prior to the pull-of test, the IOP value was measured through a rebound tonometer (FA800vet, FuAn, China; resolution: ± 1.5–2.0 mmHg) with high interobserver reliability. An Instron 5544 tester (Instron, USA) with a load cell of 5 N was employed to perform the test. The corresponding resolutions of the force and the displacement were 0.001 N and 0.001 mm, respectively. During the test, a spherical rigid punch was employed to indent the corneal tissue to 2 mN and then detach from it by 1.0 mm/min (Fig. 5b). The entire experimental course was carefully observed through capturing the images using a charge-coupled device (CCD) of DP71 (Olympus, Japan).

Previous studies have defined the adhesion behavior, as shown in Fig. 5b, it begins at that moment the punch unloads to zero force.[24–26] And its whole course can be divided into two steps, i.e., the pull-in and

the pull-off. They describe the punch detaches from the contacted cornea to the peak value of the separation force, and goes on separating from the peak force to zero force again, respectively. The peak value of the separation force is defined as the pull-off force, i.e., the adhesion force F_{ad}.

Theoretical analysis

Hertz (1896) firstly solved the contaction problem between two rigid spheres.[27] Based on the Hertz contact pressure and the indentation theory derived by Sneddon (1965)[28], Johnson et al. (1971)[6] reported the solution of the contaction between a rigid sphere and a compliance solid (Fig. S4), i.e., the JKR model (derivations in the *supplementary information* **II** and **III**). The related magnitude of the adhesion force solved by the JKR model is 1.5γπR, with $1/R = 1/R_c+1/R_p$, in this study, R_c and R_p are the radii of the cornea and the punch, respectively (Fig. 5a).

Physiologically, the surrounding of a natural cornea is inflated by the IOP. The cornea, therefore, cannot be considered as an absolute solid (Fig. 5c), yet it should be suitably considered to superimpose the contribution of the characteristic of membrane (Fig. 5d). That means to analyze the corneal adhesion, it cannot be ignored the contribution from the surface tension. Accordingly, in this study, we modified the JKR model through superposition the term of surface tension, which is formulated as follows.

$$F=\frac{4E^* a^3}{3R} - \sqrt{8\pi\gamma E^* a^3} - \alpha P\pi a^2\frac{R_c}{R_p}$$

1

,

where, a denotes the contact radius between the spherical rigid punch and the soft cornea, $E^* \approx E_c/(1-\upsilon_c^2)$ is the effective elastic modulus with E_c and υ_c being the elastic modulus and Poisson's ratio of cornea, respectively. It was assumed that the cornea was incompressible, and thus υ_c equals to 0.5. Additionally, α is a constant coefficient used to describe the degree of the cornea trending to membrane.

To obtain the corneal adhesion force F_{ad}, in mathematics, is to solve the peak value from Eq. (1). It is to find the critical contact radius a_c, in the partial differential solution of $\partial F/\partial a = 0$. And then substituting the a_c into Eq. (1), the calculated result is the obtained F_{ad} value.

In terms of Eq. (1), while α equals to zero, it describes the classical JKR solution, consists of two terms, that is, the Hertz's contact pressure[22] and the Kendall's interfacial adhesion force[29]. In this case, solving the differential equation of $\partial F/\partial a = 0$, one can obtain the value of a_c equals to $(9/8)^{1/3}\left(\gamma\pi R^2 \Big/ E^*\right)^{1/3}$. And employing this a_c into Eq. (1) with α = 0, one can solve the F_{ad} value is 1.5γπR. On the other hand, while α equals to one, Eq. (1) describes the adhesion behavior of a pure membrane material. The modified JKR model, 0 < α < 1, is hard to obtain the analytic solutions. In this study, we obtained the related numerical solutions through the software of PyCharm (JetBrains, Czech).

To solve the magnitudes of the corneal adhesion, two intrinsic characteristics of cornea, γ and E^*, should be determined. According to the previous literatures,[8,9] if a compliance material exhibits linear adhesion behavior as shown in the inset of Fig. 5b, γ can be simply formulated as $\gamma = \sigma_m \delta_m/2$, where σ_m and δ_m are the maximum adhesion stress and distance, respectively. In terms of E^*, it can be solved through the JKR solution with zero loads, i.e., the *Eq*. (S12) in *supplementary information* **III**, which is formulated as

$$a_0^3 = \frac{3R}{4E^*}(6\gamma\pi R)$$

2

,

where a_0 is the contact radius between the punch and the cornea at that moment of the experimental data transform from the unloading phase into the pull-in phase (Fig. 5b).

Data analysis

The related data were presented as **mean** ± standard deviation (**s.d.**), and were statistically analyzed through one-way analysis of variance (ANOVA) subjected to as LSD test in the help of SPSS v.24.0 (SPSS Inc). A probably value (p) of less than 0.05 was statistical different.

Declarations

Data Availability

All data generated or analysed during this study are included in this published article (and its Supplementary Information files).

Acknowledgements

This work is supported by the National Natural Science Foundation of China (Grants: 31800789, 12072218, 11872262, 12172243).

Author contributions

Z. Gao designed this work guided by Prof. X. Li and Prof. W. Chen. J. Yang, D. Zhao, and Z. Gao performed the pull-off test. J. Yang, Z. Gao, Q. Ren and R.He, analyzed the experimental data. Q. Ren and J. Yang sketched the related illustration graphs. Z. Gao derived the related theory guided by Prof. W. Chen. Z. Gao, J. Yang, and Prof. X. Li executed the writing manuscript.

Competing interests

Te authors declare no competing interests.

References

1. Riau AK, Chi LY, Yam GHF, et al. Stromal keratophakia: Corneal inlay implantation. Prog. Retin. Eye. Res. 75 (2020) 100780.
2. Yu Y, Hsu KH, Gharami S, et al. Interfacial polymerization of a thin film on contact lenses for improving lubricity. J. Colloid. Interface. Sci. 571 (2020) 356-367.
3. Zhu D, Liu Y, Gilbert JL. Micromechanical measurement of adhesion of dehydrating silicone hydrogel contact lenses to corneal tissue. Acta. Biomater. 127 (2021) 242-251.
4. Khamar P, Shetty R, Vaishnav R, et al. Biomechanics of LASIK flap and SMILE cap: a prospective, clinical study. J. Refract. Surg. 35(5) (2019) 324-332.
5. Sharifi R, Mahmoudzadeh S, Islam MM, et al. Covalent Functionalization of PMMA Surface with L-3, 4-Dihydroxyphenylalanine (L-DOPA) to Enhance its Biocompatibility and Adhesion to Corneal Tissue. Adv. Mater. Interfaces. 7(1) (2020) 1900767.
6. Johnson KL, Kendall K, Roberts AD. Surface energy and the contact of elastic solids. Proc. Math. Phys. Eng. Sci. 324 (1971) 301-313.
7. Amini R, Barocas VH. Anterior chamber angle opening during corneoscleral indentation: the mechanism of whole eye globe deformation and the importance of the limbus. Invest. Ophth. Vis. Sci. 50(11) (2009) 5288-5294.
8. Jiang Y, Grierson DS, Turner KT. Flat punch adhesion: transition from fracture-based to strength-limited pull-off. J. Phys. D. Appl. Phys. 47(32) (2014) 325301.
9. Peng B, Feng XQ, Li Q. Decohesion of a rigid flat punch from an elastic layer of finite thickness. J. Mech. Phys. Solids. 139 (2020) 103937.
10. Ren QM, Chen J, Li XN, et al. Effective elastic modulus of an intact cornea related to indentation behavior: A comparison between the Hertz model and Johnson-Kendall-Roberts model. Exp. Eye. Res. 209 (2021) 108670.
11. Johnson KL, Greenwood JA. An adhesion map for the contact of elastic spheres. J. Colloid. Interf. Sci. 192(2) (1997) 326-333.
12. Derjaguin BV, Muller VM, Toporov YP. Effect of contact deformations on the adhesion of particles. J. Colloid. Interf. Sci. 53(2) (1975) 314-326.
13. Tang T, Hui CY. Decohesion of a rigid punch from an elastic layer: Transition from “flaw sensitive” to “flaw insensitive” regime. J. Polym. Sci. Pol. Phys. 43(24) (2005) 3628-3637.
14. Ciavarella M, Joe J, Papangelo A, et al. The role of adhesion in contact mechanics. J. R. Soc. Interface. 16(151) (2019) 20180738.
15. Xia G, Huang Y, Su Y, et al. Exact axisymmetric adhesive contact analysis for a pre-deformed soft electroactive half-space. Int. J. Solids. Struct. 207 (2020) 206-229.
16. Kuhar K, Jesbeer M, Ghatak A. Soft Gel-Filled Composite Adhesive for Dry and Wet Adhesion. ACS. Appl. Polym. Mater. 3(8) (2021) 3755-3765.

17. Hu J, Youssefian S, Obayemi J, et al. Investigation of adhesive interactions in the specific targeting of Triptorelin-conjugated PEG-coated magnetite nanoparticles to breast cancer cells. Acta. Biomater. 71 (2018) 363-378.
18. Wu G, Gotthardt M, Gollasch M. Assessment of nanoindentation in stiffness measurement of soft biomaterials: kidney, liver, spleen, and uterus. Sci. Rep. 10(1) (2020) 1-11.
19. Yang W, Meyers MA, Ritchie RO. Structural architectures with toughening mechanisms in Nature: A review of the materials science of Type-I collagenous materials. Prog. Mater. Sci. 103 (2019) 425-483.
20. Qian J, Gao H. Scaling effects of wet adhesion in biological attachment systems. Acta. Biomater. 2(1) (2006) 51-58.
21. Busin M, Leon P, Nahum Y, et al. Large (9 mm) deep anterior lamellar keratoplasty with clearance of a 6-mm optical zone optimizes outcomes of keratoconus surgery. Ophthalmology 124(7) (2017) 1072-1080.
22. Zhang JH, Wang SR, He YX, et al. The best optical zone for small-incision lenticule extraction in high myopic patients. J. Cataract. Ref. Sur. 46, (2020) 1302-1307.
23. Sharifi S, Sharifi H, Guild C, et al. Toward electron-beam sterilization of a pre-assembled Boston keratoprosthesis. Ocul. Surf. 20 (2021) 176-184.
24. Lai Y, He D, Hu Y. Indentation adhesion of hydrogels over a wide range of length and time scales. Extreme. Mech. Lett. 31 (2019) 100540.
25. Li Y, Huang S, Wei C, et al. Adhesion of two-dimensional titanium carbides (MXenes) and graphene to silicon. Nat. Commun. 10(1) (2019) 1-8.
26. Deng W, Kesari H. Effect of machine stiffness on interpreting contact force–indentation depth curves in adhesive elastic contact experiments. J. Mech. Phys. Solids. 131 (2019) 404-423.
27. Hertz H. Miscellaneous papers. London: Macmillan, 1896.
28. Sneddon IN. The relation between load and penetration in the axisymmetric Boussinesq problem for a punch of arbitrary profile. Int. J. Eng. Sci. 3(1) (1965) 47-57.
29. Kendall K. The adhesion and surface energy of elastic solids. J. Phys. D. Appl. Phys. 4(8) (1971) 1186.

Figures

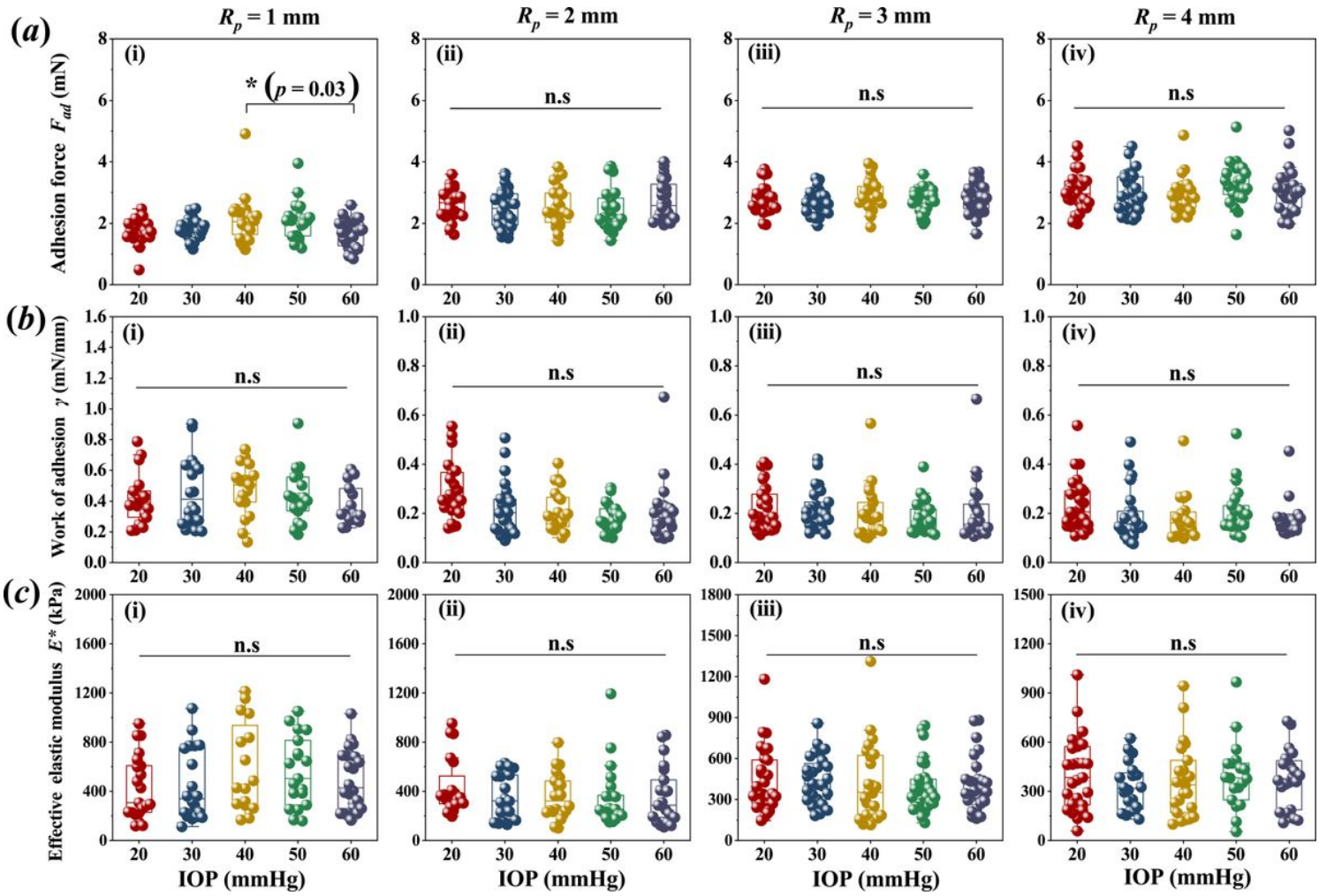

Figure 1

Parameters obtained from the experiment. (**a**) adhesion force F_{ad}, (**b**) work of adhesion γ, and (**c**) effective elastic modulus E^*, respectively (the data signed by **n.s** indicate no statistical differences among the different groups with $p > 0.05$ and signed by * indicate $p < 0.05$).

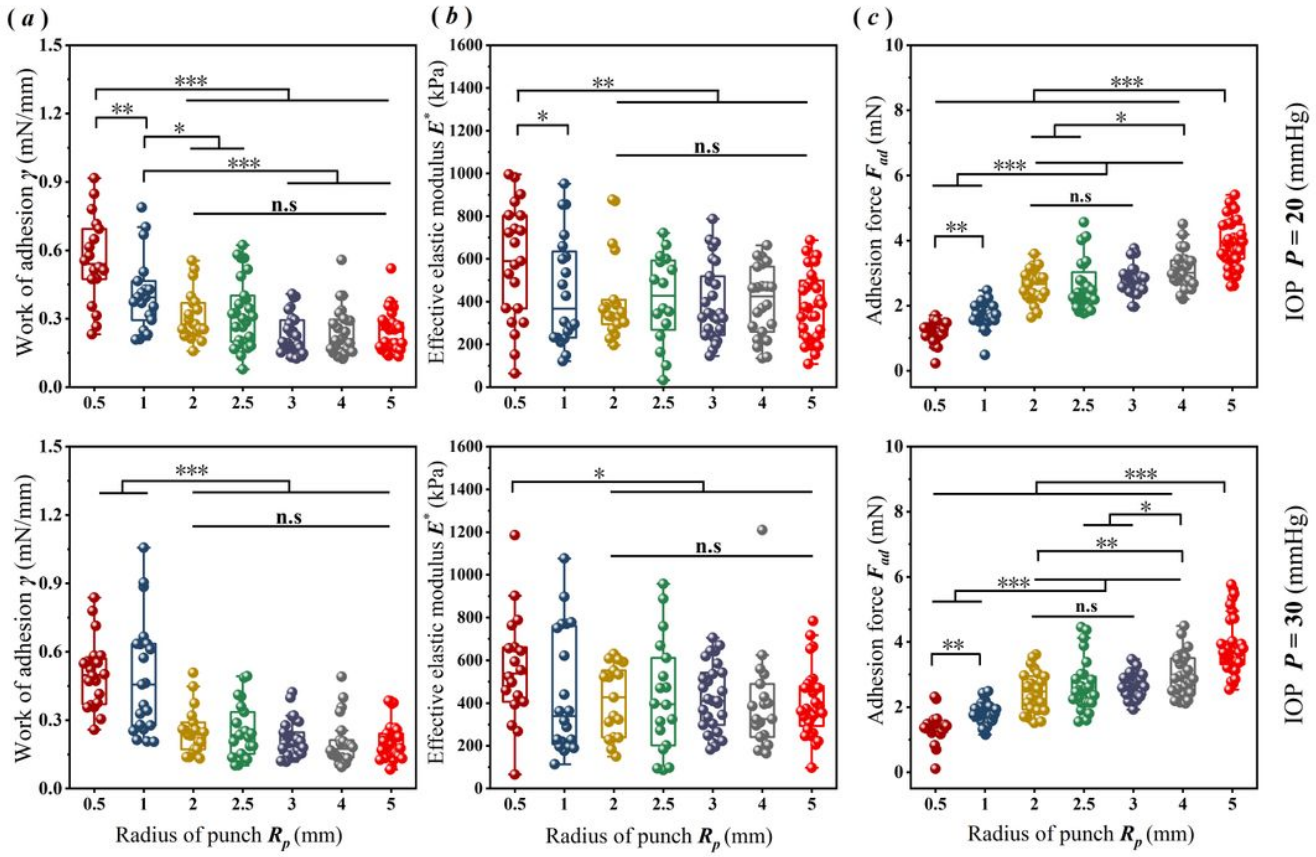

Figure 2

Scale effect of corneal adhesion. (**a**) work of adhesion γ, (**b**) effective elastic modulus E^*, and (**c**) adhesion force F_{ad} under the normal IOP of 20 mmHg and 30 mmHg, respectively (the data signed by * indicate $p < 0.05$, ** indicate $p < 0.01$, and *** indicate $p < 0.001$, respectively; and signed by **n.s** indicate no statistical differences among the groups with $p > 0.05$).

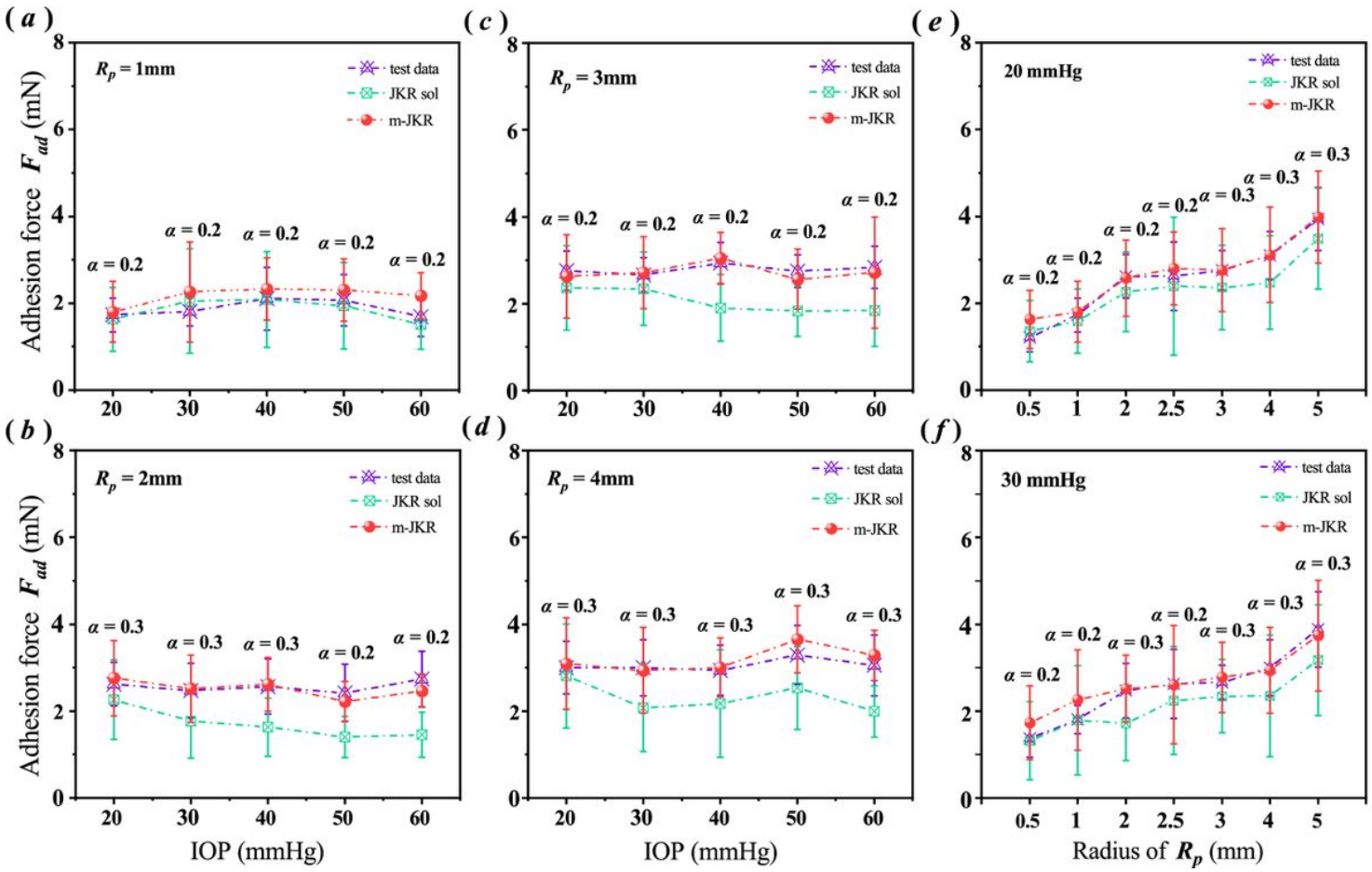

Figure 3

Comparisons of the corneal adhesion force F_{ad} obtained from the experiment and theories. (**a**)-(**d**) show the comparisons with different IOPs. (**e**)-(**f**) show the comparisons of the scale effect of the corneal adhesion under the normal IOP of 20 mmHg and 30 mmHg (the data presented as **mean** ± **s.d.**, and the abbreviations of JKR sol and m-JKR indicate the solutions from JKR and modified-JKR models, respectively).

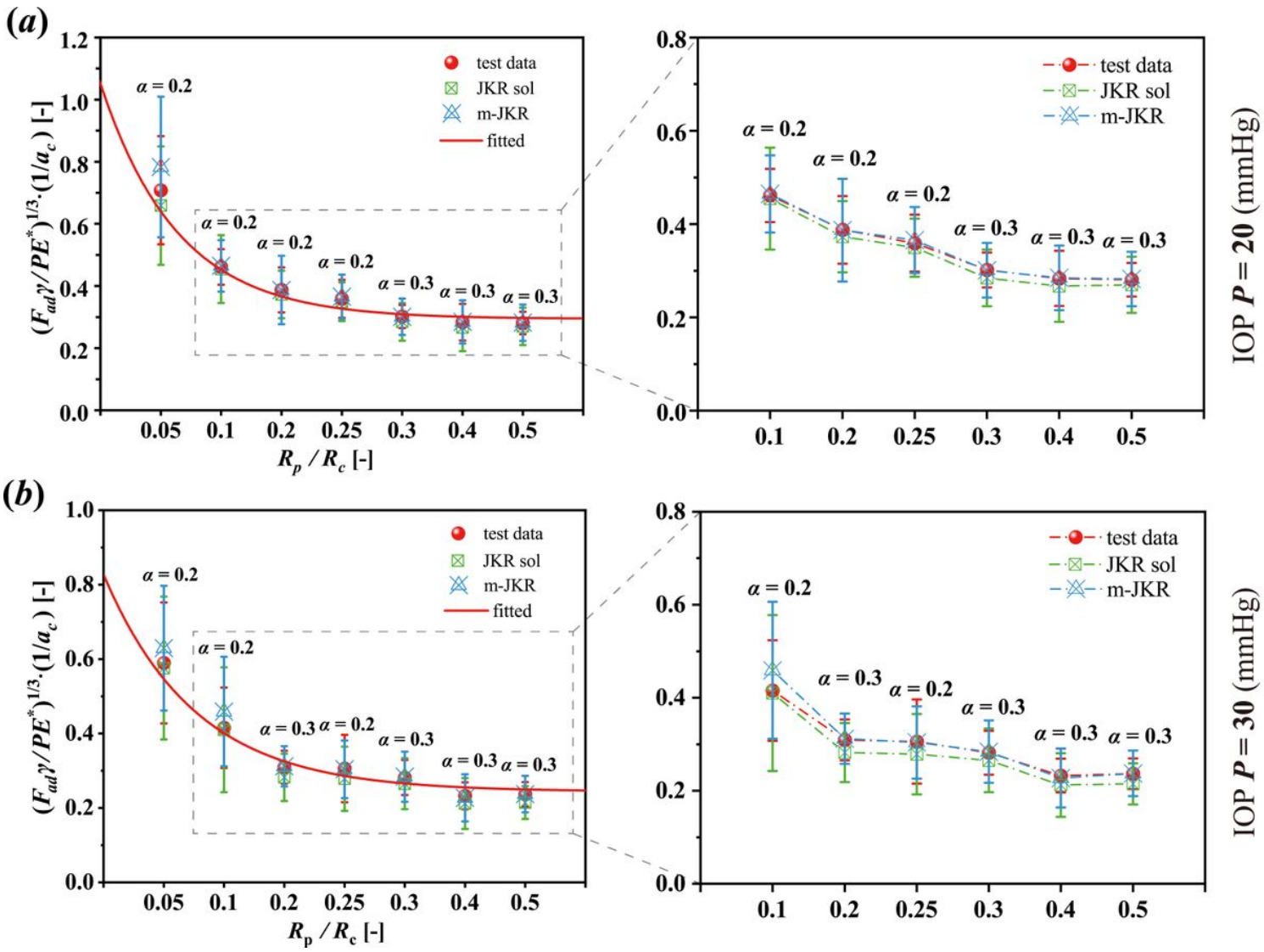

Figure 4

Normalization analysis of the scale effect of corneal adhesion. (**a**) under 20 mmHg, the fitting exponential function is $y = 0.76\ exp\ (-12.53x) + 0.29$, (**b**) under 30 mmHg, the fitting exponential function is $y = 0.58\ exp\ (-10.49x) + 0.24$ (the data presented as **mean** ± **s.d.**, and the abbreviations of JKR sol and m-JKR indicate the solutions from JKR and modified-JKR models, respectively).

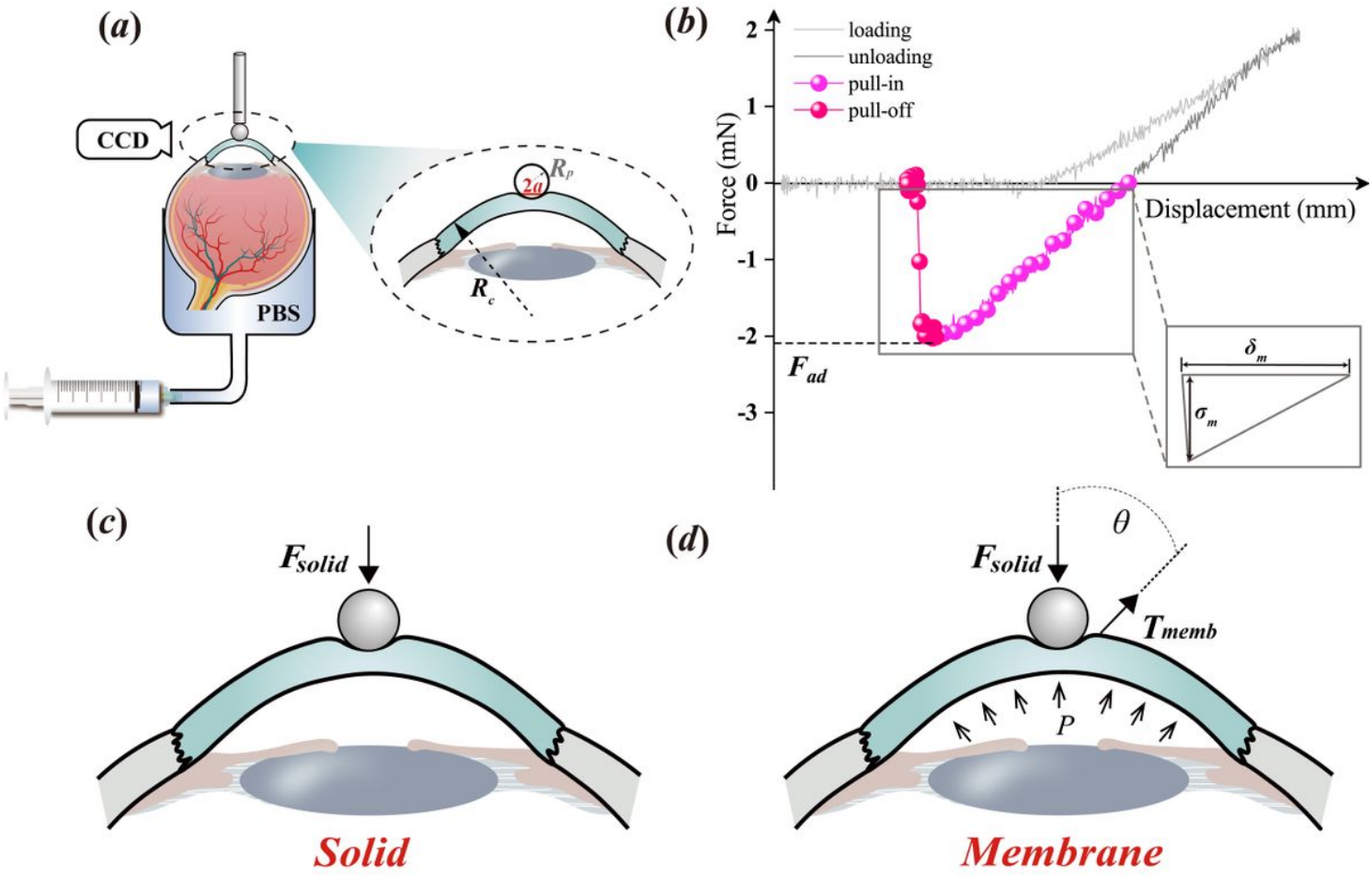

Figure 5

Schematic illustrations for determining the corneal adhesion. (**a**) Sketching of the pull-off test, in which R_p and R_c respectively represent the radii of the punch and the cornea, and a is the related contact radius. (**b**) An example of the experimental data. (**c**) and (**d**) Sketching for illustrating the related analysis theory, in which F_{solid} represents the adhesion force balanced by the Hertz and the Knedall terms and T_{memb} represents the surface tension related to the membrane characteristic.

Supplementary Files

This is a list of supplementary files associated with this preprint. Click to download.

- Supplementary.docx